RSC Advances

PAPER

View Article Online
View Journal | View Issue



Cite this: *RSC Adv.*, 2024, **14**, 10761

# Multicomponent synthesis *via* acceptorless alcohol dehydrogenation: an easy access to tri-substituted pyridines†

Hima P., Vageesh M. and Raju Dey *

Herein, we report palladium supported on a hydroxyapatite catalyst for synthesizing tri-substituted pyridines using ammonium acetate as the nitrogen source *via* acceptorless alcohol dehydrogenation strategy. The strategy offers a broad substrate scope using inexpensive and readily available alcohols as the starting material. The catalyst was prepared using a simple method and analyzed by several techniques, including FE-SEM, EDS, HR-TEM, BET, XRD, FT-IR, UV-visible spectroscopy, and XPS, demonstrating the anchoring of Pd nanoparticles on hydroxyapatite in the zero oxidation state. Moreover, several controlled experiments were carried out to understand the reaction pathway and a suitable mechanism has been proposed.

Received 17th January 2024
Accepted 6th March 2024

DOI: 10.1039/d4ra00439f

rsc.li/rsc-advances



The synthesis of N-heterocycles has attracted incredible attention considering their inevitable role in natural products,[1] pharmaceuticals,[2] agrochemicals,[3] and functional materials.[4] Among other N-heterocycles, pyridine-containing compounds have high significance owing to their numerous applications as biomolecules, organocatalysts, ligands, linkers, and sensors (Fig. 1).[5] Thus, functionalizing the pyridine moiety offers an attractive method for synthesizing interesting compounds with diverse applications.[6] Several methods have been reported for synthesizing pyridine derivatives, including classical condensation reactions,[7] C–H annulation reactions,[8] and multicomponent approaches.[9] However, most of these methods have drawbacks, such as poor atom economy,[10] generation of large amounts of waste,[11] and harsh reaction conditions.[12]

Since the last decade, acceptorless dehydrogenative coupling (ADC) reactions have emerged as an efficient methodology for synthesizing diverse heterocyclic compounds from relatively inexpensive and readily available starting materials.[13] In this strategy, the by-products generated are hydrogen and water, which make these methods environmentally benign with a high atom economy.[14] Acceptorless alcohol dehydrogenation has garnered attention because of the easy availability of inexpensive and less toxic alcohols as the starting material.[15] Thus, several research groups are engaged in exploring acceptorless alcohol dehydrogenation strategies for the synthesis of various heterocyclic compounds.[16] In 2013, Milstein and co-workers reported on the ruthenium-catalyzed synthesis of 2,6-disubstituted pyridines using γ-amino-alcohols with secondary alcohols.[17]

Later, Kempe and his group synthesized 3-aminopyridines *via* the Ir-catalyzed dehydrogenative coupling of γ-amino alcohols and β-amino alcohols.[18] These methods were found to be very interesting and remarkable. However, the use of air-sensitive phosphine-based ligands limited their applications.

An interesting report by Deng *et al.* revealed a strategy for synthesizing tri-substituted pyridine through the condensation of aldehyde, methyl ketone, and ammonium salts under air (Scheme 1a).[19] Recently, Paul and co-workers reported a similar approach using alcohols as the primary feedstock catalyzed by an air-stable Zn(II)-catalyst, featuring a redox-active tridentate azo-aromatic pincer, 2-((4-chlorophenyl)diazenyl)-1,10-phenanthroline, for synthesizing 2,4,6-trisubstituted pyridine

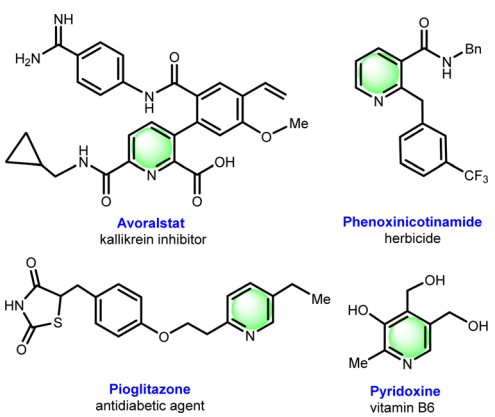


Fig. 1 Selected examples of pyridine-containing molecules having a wide range of applications.

*Department of Chemistry, National Institute of Technology Calicut, Kozhikode, 673601, India. E-mail: rajudey@nitc.ac.in*

† Electronic supplementary information (ESI) available: General information, experimental procedure, catalyst characterization data, $^{1}$H NMR, and $^{13}$C NMR spectral data of all compounds. See DOI: https://doi.org/10.1039/d4ra00439f

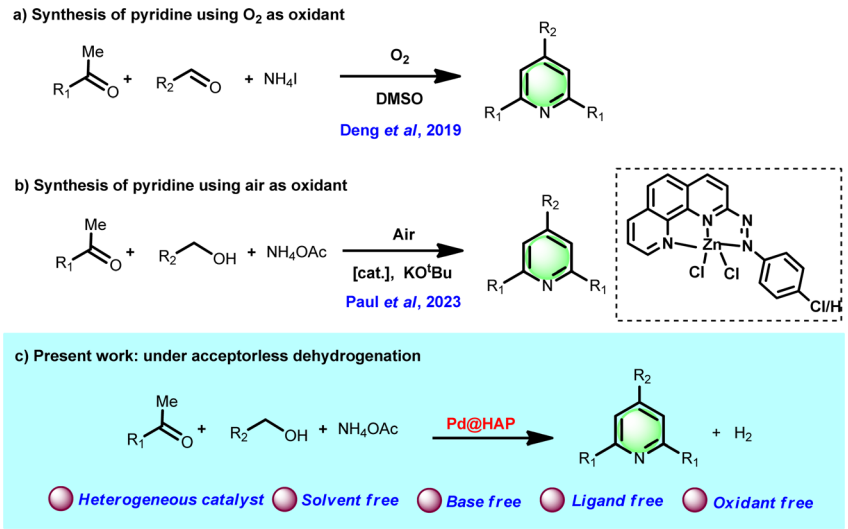


Scheme 1 Context of the study.

(Scheme 1b).[20] The aforesaid method works well under homogeneous reaction conditions.

Heterogeneous catalysis plays a pivotal role in numerous chemical and industrial processes[21] and has gained wide attention considering its remarkable ability to accelerate reaction rates, low cost, higher stability, and selectivity.[22] Moreover, their ease of separation, reusable nature, and benign character make heterogeneous catalysts an appropriate choice for the sustainable synthesis of organic compounds.[23] In this regard, hydroxyapatite, a biomaterial, has received significant importance for its utility as a heterogeneous support.[24] Transition metals supported on the hydroxyapatite surface show efficient catalytic performances in a variety of organic transformations.[25] Among others, hydroxyapatite-supported metal nano-catalysts have been less explored for the synthesis of heterocycles *via* acceptorless alcohol dehydrogenation methodology.[26]

Recently, our group reported on a hydroxyapatite-supported copper nano-catalyst for direct C($sp^3$)-S coupling between alcohols and dithiocarbamate anions *via* the borrowing hydrogen strategy.[27a] With our continued interest in exploring the novel applications of acceptorless dehydrogenation reactions,[27] we report here palladium supported on a hydroxyapatite catalyst for the synthesis of tri-substituted pyridines using ammonium acetate as the nitrogen source *via* an acceptorless alcohol dehydrogenation strategy.

## Result and discussion

The catalyst was prepared using the wet impregnation method. Initially, $PdCl_2$ was dissolved in 5 mL of aqueous NaCl (0.2 M) solution, resulting in a brown coloration, and was added dropwise into a stirring slurry of hydroxyapatite at room temperature. Then, the pH was adjusted to 11 using a concentrated ammonia solution, and the mixture was stirred for 24 h at room temperature.

At this time, the aqueous supernatant becomes colorless, indicating the complete anchoring of Pd(II) onto the support. The light brown Pd(II) HAP is then reduced by $NaBH_4$ and results in a solid black residue. The black residue is then washed with distilled water thoroughly and dried at 70 °C overnight to give the grey-black powder Pd NPs@HAP with metal loading (0.6 wt%) found by ICP-MS analysis, and labelled as Pd NPs@HAP (Scheme S1 and S3 in ESI†).

The synthesized Pd NPs@HAP was then characterized using various spectroscopic and analytical techniques, including FE-SEM, HR-TEM, XPS, *p*-XRD, FT-IR, UV-visible spectroscopy, and BET analysis. The nitrogen adsorption–desorption isotherm plot was classified as type IV, and the surface area calculated by the BET method was 86.496 $m^2\ g^{-1}$ (Fig. S1, ESI†). Moreover, the pore size and pore volume were found to be 30.004 nm and 0.6488 $cm^3\ g^{-1}$, respectively (Table S1, ESI†). The energy-dispersive spectroscopy (EDS) analysis of Pd NPs@HAP was performed along with SEM analysis in different selected zones of the Pd NPs@HAP surface, confirming the presence of elemental Ca, Cu, P, O and Pd (Fig. S2, ESI†).

TEM images show the presence of homogeneously distributed palladium nanoparticles on the HAP surface (Fig. 2a–c). The sizes of the particles are in the range of 10–20 nm. The high-resolution TEM image of Pd NPs@HAP shows the high crystallinity of the palladium (0) nanoparticles, and the crystalline spacing of 0.2 nm agrees with the [111] lattice spacing of palladium.[28] The crystallinity and structural composition of the synthesized materials were ensured by X-ray diffraction (XRD) analysis at room temperature (Fig. S4a, ESI†). Powder XRD diffraction patterns of Pd NPs@HAP exhibited a broad reflection, corresponding to the hydroxyapatite support. Three additional reflections were found in the XRD pattern ($2\theta = 39°$, 46° and 65°), which could be attributed to Pd(0).[29] The FTIR spectra of HAP and Pd NPs@HAP show the characteristic tetrahedral $PO_4^{3-}$ peaks, which are at 472–600 $cm^{-1}$ and 1032–1090 $cm^{-1}$ (Fig. S4b, ESI†).[30]

The elemental analysis and chemical states of palladium on the surface of the Pd NPs@HAP catalyst were determined by XPS analysis (Fig. 2d and e). The XPS spectra of Ca 2p, P 2p, and O 1s

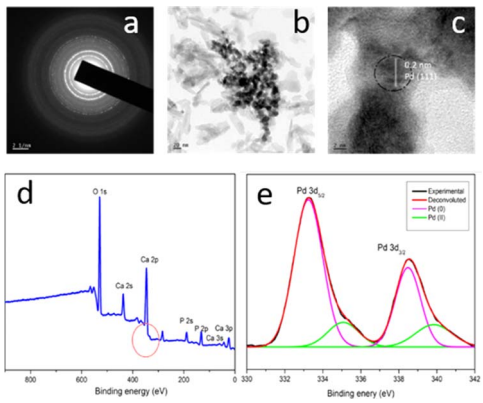


Fig. 2 (a) SAED patterns of Pd NPs@HAP. (b) HR-TEM image of Pd NPs@HAP. (c) High-magnification HR-TEM image of Pd NPs@HAP showing the palladium nanoparticle with an average size of 10–20 nm and lattice plane of 0.2 nm, which corresponds to the palladium of the (111) plane. (d) XPS elemental analysis of Pd NPs@HAP shows the support hydroxyapatite composed of calcium, phosphorous, and oxygen. (e) Binding energy value for Pd in Pd NPs@HAP.

are characteristic of phosphorus, calcium, and oxygen in hydroxyapatite. The 2p peaks at 133.8 eV and 132.9 eV are assigned to the phosphorus in hydroxyapatite. The Ca 2p spectra are composed of two peaks corresponding to Ca $2p_{1/2}$ and Ca $2p_{3/2}$. The binding energy of O 1s consists of two peaks at 531.62 eV and 530.92 eV associated with the presence of O–P and O–H groups in hydroxyapatite, respectively. The binding energy analysis of Pd revealed two predominant distinct Pd 3d doublets ($3d_{5/2}$ and $3d_{3/2}$) at 335.3 eV and 340.6 eV, indicative of Pd (0).[31] Palladium nanoparticle formation has been further investigated using UV-visible spectroscopy in the 200–800 nm range. The absence of absorption peaks above 300 nm in all of the samples shows the full reduction of the initial Pd(II) ions and the formation of Pd(0) nanoparticles.

After the detailed characterization of the catalyst, Pd NPs@HAP was then tested for the synthesis of tri-substituted pyridines using ammonium acetate as the nitrogen source *via* an acceptorless alcohol dehydrogenation strategy. The aryl methyl ketone, primary alcohol, $NH_4OAC$ was heated in the presence of the Pd NPs@HAP catalyst at 150 °C in a Teflon-lined pressure tube under neat conditions. Upon completion of the reaction (by TLC), the crude product is purified by column chromatography. The reaction was studied with various parameters, such as the reaction temperature, time, and catalyst to optimize the reaction conditions, and the results are summarized in Table 1.

It was found that the product formation was complete at 150 °C (Table 1, entry 3). The reaction was incomplete at temperatures below the optimal temperature (Table 1, entries 1 and 2) and no reaction at room temperature (Table 1, entry 5). Moreover, a minimum of 24 h reaction time was required to complete the reaction (Table 1, entry 4). As expected, in the absence of the Pd NPs@HAP catalyst, we were unable to detect any product (Table 1, entry 7). Similarly, $PdCl_2$ or HAP alone failed to carry out any reaction (Table 1, entries 9 and 11). The catalyst precursor Pd(II)@HAP generated only a trace amount of the product (Table 1, entry 8), which indicates the role of Pd(0) NPs in the reaction mechanism. On the other hand, $Pd(PPh_3)_4$

Table 1 Optimization of the reaction conditions[a]

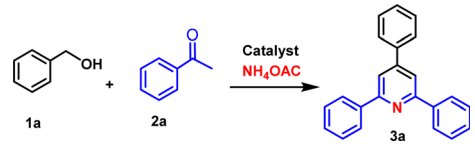


| Entry | Catalyst | Temperature (°C) | Time (h) | Conversion[b,c] (%) |
|---|---|---|---|---|
| 1 | Pd NPs@HAP | 100 | 24 | 30 |
| 2 | Pd NPs@HAP | 130 | 24 | 42 |
| 3 | Pd NPs@HAP | 150 | 24 | 95 |
| 4 | Pd NPs@HAP | 150 | 12 | 58 |
| 5 | Pd NPs@HAP | Rt | 24 | Nd |
| 6 | Pd NPs@HAP | 150 | 24 | 30[d] |
| 7 | — | 150 | 24 | Nd |
| 8 | $Pd^{II}$@HAP | 150 | 24 | 15 |
| 9 | $PdCl_2$ | 150 | 24 | Nd |
| 10 | $Pd(PPh_3)_4$ | 150 | 24 | 10 |
| 11 | HAP | 130 | 24 | Nd |

[a] Reaction condition: benzyl alcohol (0.25 mmol), acetophenone (0.6 mmol), catalyst (25 mg, Pd loading 0.6 wt%), stirred for required time using a Teflon-lined pressure tube on a preheated heating block. [b] Conversion was calculated from $^1H$ NMR using 1,4-dimethoxy benzene as the internal standard. [c] Nd: not detected. [d] Catalyst (10 mg).

Table 2 Substrate scope for ketones [a,b]

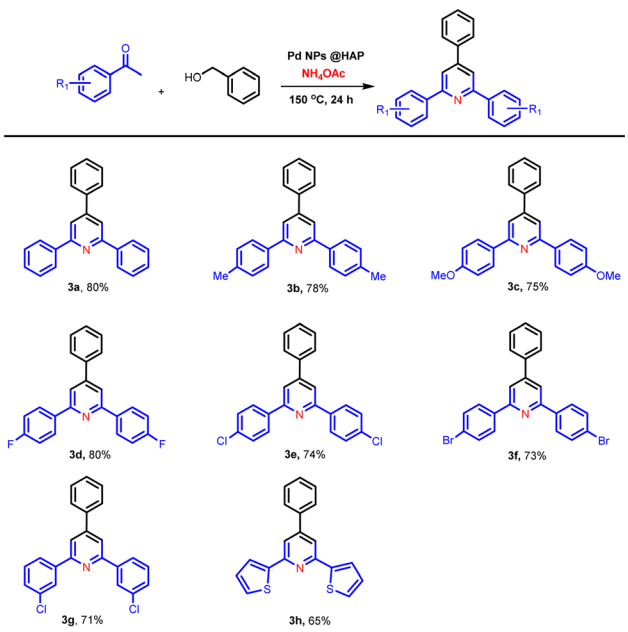


[a] Reaction condition: benzyl alcohol (0.25 mmol), acetophenone (0.6 mmol), catalyst (25 mg, Pd loading 0.6 wt%), stirred for 24 h using a Teflon-lined pressure tube on a preheated heating block at 150 °C. [b] Yields refer to those of pure products characterized by $^1H$ NMR and $^{13}C$ NMR spectroscopic data.

Table 3 Substrate scope for alcohols[a,b]

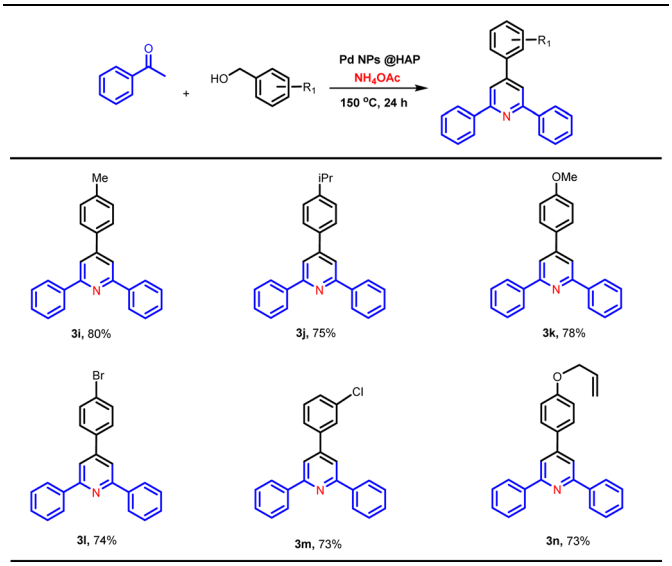


[a] Reaction condition: benzyl alcohol (0.25 mmol), acetophenone (0.6 mmol), catalyst (25 mg, Pd loading 0.6 wt%), stirred for 24 h using a Teflon-lined pressure tube on a preheated heating block at 150 °C. [b] Yields refer to those of pure products characterized by $^1$H NMR and $^{13}$C NMR spectroscopic data.

failed to generate even the marginal conversion (Table 1, entry 10). The maximum yield of the product was obtained when we carried out the reaction using Pd NPs@HAP at 150 °C (heating block temperature) in a Teflon-lined pressure tube under neat conditions for 24 h (Table 1, entry 3).

Using the optimized condition, we have synthesized several 2,4,6 tri-substituted pyridines *via* multicomponent dehydrogenative coupling of benzyl alcohols and aryl methyl ketones with $NH_4OAc$ as the nitrogen source. Acetophenones bearing various functional groups performed well in this reaction (Table 2). Additionally, *p*-Me, *p*-OMe gave a similar yield as that of the unsubstituted acetophenone (Table 2, **3b** and **3c**) and resulted in the corresponding tri-substituted pyridine with 70–80% yield. Similarly, *para*-substituted halogen derivatives also gave the desired product in good yields without affecting the halogen functionality (Table 2, **3d**, **3e**, and **3f**). Interestingly, heterocyclic moieties bearing the acetyl group also performed well (Table 2, **3h**), and gave the corresponding product with 65% yield. Surprisingly, the highly electron-withdrawing 4-nitro acetophenone, as well as aliphatic methyl ketones, failed to give the desired product under this protocol.

After exploring various acetophenones, we then checked the performance of different alcohols for this synthesis (Table 3). Various benzylic alcohols undergo this reaction with good performance, and we isolated the corresponding tri-substituted pyridine with 70–75% yield.

4-Methyl benzyl alcohol and 4-isopropyl benzyl alcohol underwent the reaction smoothly, and resulted in 79–80% yields of the desired products (Table 3, **3i** and **3j**). Similarly, 4-OMe substituted benzyl alcohol also resulted in 75% yield of the anticipated product (Table 3, **3k**). Halogen-substituted benzyl alcohol underwent the reaction easily (Table 3, **3l** and **3m**). Moreover, the easily hydrolyzable 4-(allyloxy)benzyl alcohol also gave the corresponding pyridine selectively (Table 3, **3n**). The 4-nitrobenzyl alcohol and aliphatic alcohols failed to give the product as in the previous case.

After exploring the substrate scope for alcohols and methyl ketones, we studied the mechanism of the reaction. To analyze the mechanism, we carried out various controlled experiments (Scheme 2). When we carried out the reaction only with benzyl alcohol in the presence of Pd NPs@HAP, we isolated benzaldehyde and detected hydrogen by gas chromatography (Scheme 2a and Fig. S6†). This confirms the formation of benzaldehyde as the intermediate. Similarly, when we performed the reaction

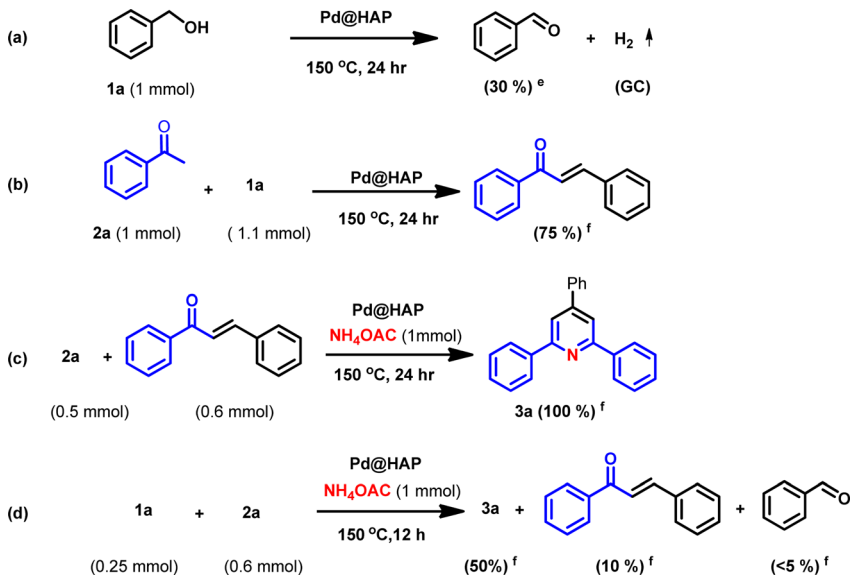


Scheme 2 Controlled experiments ([e]isolated yield, [f]conversion was calculated from $^1$H NMR using a crude reaction mixture).

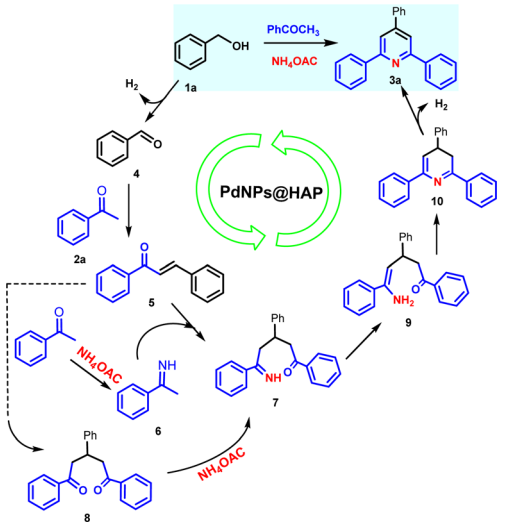


Scheme 3 Proposed mechanism.

without $NH_4OAC$, we confirmed the corresponding chalcone as the product (Scheme 2b). Furthermore, to confirm chalcone as the intermediate, we performed a reaction using synthesized chalcone and $NH_4OAC$ under the same condition, which resulted in the corresponding trisubstituted pyridine in 100% conversion (Scheme 2c). Moreover, the crude $^1H$ NMR after the half interval of the reaction showed the formation of benzaldehyde and chalcone as the reaction intermediate (Scheme 2d).

From all these experiments and available literature, we have proposed a suitable mechanism for the transformation. The proposed mechanism is depicted in Scheme 3. Initially, the Pd@HAP-catalyzed dehydrogenation of alcohol resulted in the formation of benzaldehyde, which is coupled with methyl ketone, and generates the corresponding α,β-unsaturated ketone. Meanwhile, the second molecule of ketone reacts with ammonium acetate, forming the corresponding imine. Further condensation of the formed imine and α,β-unsaturated ketone, followed by cyclization, produces the desired 2,4,6-trisubstituted pyridine as the final product. Moreover, there was no significant difference in the yield obtained when we carried out the reaction in the presence of metallic mercury (mercury poisoning test), ruling out the leaching of metallic Pd from the HAP support. However, during catalyst recyclability, it has been observed that the catalyst efficiency slowly decreased (Fig. S7†). Metal contamination in the final product was checked by ICP-MS, and was found to be less than 1 microgram of palladium per gram of product, which is within the acceptable limit for pharmaceutical application.[32]

## Conclusion

In conclusion, we have reported on palladium nanoparticles supported on hydroxyapatite as the catalyst for the synthesis of tri-substituted pyridines using ammonium acetate as the nitrogen source *via* an acceptorless alcohol dehydrogenation strategy. The present methodology has wide functional group tolerance, and offers general applicability for the synthesis of a variety of tri-substituted pyridine derivatives in an environmentally benign route. This methodology offers other important advantages, such as avoiding toxic ligands and bases, use of a biocompatible material as the catalyst support, operational simplicity, among other advantages. To the best of our knowledge, this is the first report of direct tri-substituted pyridine synthesis *via* acceptorless alcohol dehydrogenation using $NH_4OAC$ as the ammonia source catalyzed by a supported metal catalyst.

## Conflicts of interest

The authors declare no competing financial interest.

## Acknowledgements

R. D. acknowledges the Science and Engineering Research Board (SRG/2020/002161) India for funding. H. P. and V. M. are thankful to NIT Calicut for their fellowship.

## References

1 (*a*) D. O. Hagan, Pyrrole, pyrrolidine, pyridine, piperidine and tropane alkaloids, *Nat. Prod. Rep.*, 2000, **17**, 435–446; (*b*) B. Gao, B. Yang, X. Feng and C. Li, Recent advances in the biosynthesis strategies of nitrogen heterocyclic natural product, *Nat. Prod. Rep.*, 2022, **39**, 139–162.

2 (*a*) Z. Zeng, C. Liao and L. Yu, Molecules for COVID-19 treatment, *Chin. Chem. Lett.*, 2023, **34**, 109349; (*b*) N. Kerru, L. Gummidi, S. Maddila, K. K. Gangu and S. B. Jonnalagadda, A Review on recent advances in nitrogen-containing molecules and their biological applications, *Molecules*, 2020, **25**, 1909.

3 Y. Sanemitsu and S. Kawamura, Studies on the synthetic development for the discovery of novel heterocyclic agrochemicals, *J. Pestic. Sci.*, 2008, **33**, 175–177.

4 C. Verma, K. Y. Rhee, M. A. Quraishi and E. E. Ebenso, Pyridine based N-heterocyclic compounds as aqueous phase corrosion inhibitors: A review, *J. Taiwan Inst. Chem.*, 2020, **117**, 265–277.

5 (*a*) A. Basnet, P. Thapa, R. Karki, Y. Na, Y. Jahng, B. S. Jeong, T. C. Jeong, C. S. Lee and E. S. Lee II, 4,6-Trisubstituted pyridines: Synthesis, topoisomerase I and II inhibitory activity, cytotoxicity, and structure–activity relationship, *Bioorg. Med. Chem.*, 2007, **15**, 4351–4359; (*b*) V. V. Zakharychev, A. V. Kuzenkov and A. M. Martsynkevich, Good pyridine hunting: a biomimic compound, a modifier and a unique pharmacophore in agrochemicals, *Chem. Heterocycl. Compd.*, 2020, **56**, 1491–1516; (*c*) G. M. Abu-Taweel, M. M. Ibrahim, S. Khan, H. M. Al-Saidi, M. Alshamrani, F. A. Alhumaydhi and S. S. Alharthi, Medicinal importance and chemosensing applications of pyridine derivatives: A review, *Crit. Rev. Anal. Chem.*, 2022, 1–18.

6 P. Singh, *Recent Developments in the Synthesis and Applications of Pyridines*, Elsevier, 2023, ISBN 9780323912211.

7 (*a*) R. S. Rohokale, B. Koenig and D. D. Dhavale, Synthesis of 2,4,6-trisubstituted pyridines by oxidative Eosin Y photoredox catalysis, *J. Org. Chem.*, 2016, **81**, 7121–7126; (*b*) K. Gopalaiah, D. C. Rao, K. Mahiya and A. Tiwari, Iron-catalyzed aerobic oxidative cleavage and construction of C–N bonds: A facile method for synthesis of 2,4,6-trisubstituted pyridines, *Asian J. Org. Chem.*, 2018, **7**, 1872–1881; (*c*) Q. Yang, Y. Zhang, W. Zeng, Z. C. Duan, X. Sang and D. Wang, Merrifield resin-supported quinone as an efficient biomimetic catalyst for metal-free, base-free, chemoselective synthesis of 2, 4, 6-trisubstituted pyridines, *Green Chem.*, 2019, **21**, 5683–5690.

8 M. C. Bagley, C. Glover and E. A. Merritt, The Bohlmann-Rahtz pyridine synthesis: From discovery to applications, *Synlett*, 2007, **16**, 2459–2482.

9 C. R. Reddy, S. A. Panda and M. D. Reddy, Aza-annulation of enynyl azides: A new approach to substituted pyridines, *Org. Lett.*, 2015, **17**, 896–899.

10 X. J. Wu, R. Jiang, X. P. Xu, X. M. Su, W. H. Lu and S. J. Ji, Practical Multi-component synthesis of di- or tri-aryl (heteraryl) substituted 2-(pyridin-2-yl)imidazoles from simple building blocks, *J. Comb. Chem.*, 2010, **12**, 829–835.

11 L. Y. Fu, J. Ying and X. F. Wu, Cobalt-catalyzed carbonylative synthesis of phthalimides from *N*-(pyridin-2-ylmethyl) benzamides with TFBen as the CO source, *J. Org. Chem.*, 2019, **84**, 12648–12655.

12 R. Morgentin, F. Jung, M. Lamorlette, M. Maudet, M. Ménard, P. Plé, G. Pasquet and F. Renaud, An efficient large-scale synthesis of alkyl 5-hydroxy-pyridin- and pyrimidin-2-yl acetate, *Tetrahedron*, 2009, **65**, 757–764.

13 K. Sun, H. Shan, G. P. Lu, C. Cai and M. Beller, Synthesis of N-heterocycles *via* oxidant-free dehydrocyclization of alcohols using heterogeneous catalysts, *Angew. Chem., Int. Ed.*, 2021, **133**, 25392–25406.

14 (*a*) S. Elangovan, J. Neumann, J. B Sortais, K. Junge, C. Darcel and M. Beller, Efficient and selective *N*-alkylation of amines with alcohols catalysed by manganese pincer complexes, *Nat. Commun.*, 2016, **7**, 12641; (*b*) S. Waiba and B. Maji, Manganese catalyzed acceptorless dehydrogenative coupling reactions, *ChemCatChem*, 2019, **12**, 1891; (*c*) A. Mukherjee, A. Nerush, G. Leitus, L. J. W Shimon, Y. B. David, N. A. E. Jalapa and D. Milstein, Manganese-catalyzed environmentally benign dehydrogenative coupling of alcohols and amines to form aldimines and $H_2$: A catalytic and mechanistic study, *J. Am. Chem. Soc.*, 2016, **138**, 4298; (*d*) M. Mastalir, M. Glatz, E. Pittenauer, G. Allmaier and K. Kirchner, Sustainable synthesis of quinolines and pyrimidines catalyzed by manganese PNP pincer complexes, *J. Am. Chem. Soc.*, 2016, **138**, 15543; (*e*) N. Deibl and R. Kempe, Manganese-catalyzed multicomponent synthesis of pyrimidines from alcohols and amidines, *Angew. Chem., Int. Ed.*, 2017, **56**, 1663.

15 (*a*) G. Jaiswal, V. G. Landge, D. Jagadeesan and E. Balaraman, Iron-based nanocatalyst for the acceptorless dehydrogenation reactions, *Nat. Commun.*, 2017, **8**, 2147; (*b*) S. Chakraborty, P. E. Piszel, W. W. Brennessel and W. D. Jones, A single nickel catalyst for the acceptorless dehydrogenation of alcohols and hydrogenation of carbonyl compounds, *Organometallics*, 2015, **34**, 5203; (*c*) G. Zhang and S. K. Hanson, Cobalt-catalyzed acceptorless alcohol dehydrogenation: Synthesis of imines from alcohols and amines, *Org. Lett.*, 2013, **15**(3), 650–653.

16 (*a*) K. Chakrabarti, M. Maji and S. Kundu, Cooperative iridium complex-catalyzed synthesis of quinoxalines, benzimidazoles and quinazolines in water, *Green Chem.*, 2019, **21**, 1999–2004; (*b*) S. Das, D. Maiti and S. D. Sarkar, Synthesis of polysubstituted quinolines from α-2-aminoaryl alcohols *via* nickel-catalyzed dehydrogenative coupling, *J. Org. Chem.*, 2018, **83**, 2309–2316; (*c*) M. Maji, K. Chakrabarti, B. Paul, B. C. Roy and S. Kundu, Ruthenium(II)-NNN-pincer-complex-catalyzed reactions between various alcohols and amines for sustainable C–N and C–C bond formation, *Adv. Synth. Catal.*, 2018, **360**, 722–729.

17 D. Srimani, Y. Ben-David and D. Milstein, Direct synthesis of pyridines and quinolines by coupling of γ-amino-alcohols with secondary alcohols liberating $H_2$ catalyzed by ruthenium pincer complexes, *Chem. Commun.*, 2013, **49**, 6632–6634.

18 T. Hille, T. Irrgang and R. Kempe, Synthesis of meta-functionalized pyridines by selective dehydrogenative heterocondensation of β-and γ-amino alcohols, *Angew. Chem., Int. Ed.*, 2017, **56**, 371–374.

19 J. Chen, H. Meng, F. Zhang, F. Xiao and G. J. Deng, Transition-metal-free selective pyrimidines and pyridines formation from aromatic ketones, aldehydes and ammonium salts, *Green Chem.*, 2019, **21**, 5201–5206.

20 S. Pal, S. Das, S. Chakraborty, S. Khanra and N. D. Paul, Zn(II)-catalyzed multicomponent sustainable synthesis of pyridines in air, *J. Org. Chem.*, 2023, **88**, 3650–3665.

21 J. Heveling, Heterogeneous catalytic chemistry by example of industrial applications, *J. Chem. Educ.*, 2012, **89**, 1530–1536.

22 (*a*) D. K. Jambhulkar, R. P. Ugwekar, B. A. Bhanvase and D. P. Barai, A review on solid base heterogeneous catalysts: preparation, characterization and applications, *Chem. Eng. Commun.*, 2022, **209**, 433–484; (*b*) L. Yin and J. Liebscher, Carbon–carbon coupling reactions catalyzed by heterogeneous palladium catalysts, *Chem. Rev.*, 2007, **107**, 133–173.

23 (*a*) J. G. de Vries and S. D. Jackson, Homogeneous and heterogeneous catalysis in industry, *Catal. Sci. Technol.*, 2012, **2**, 2009; (*b*) A. Alagumalai, O. Mahian, F. Hollmann and W. Zhang, Environmentally benign solid catalysts for sustainable biodiesel production: A critical review, *Sci. Total Environ.*, 2021, **768**, 144856; (*c*) Z. Zeng, Y. Chen, X. Zhu and L. Yu, Polyaniline-supported nano metal-catalyzed coupling reactions: Opportunities and challenges, *Chin. Chem. Lett.*, 2023, **34**, 107728; (*d*) C. J. Li, G. C. Shan, C. X. Guo and R. G. Ma, Design strategies of Pd-based electrocatalysts for efficient oxygen reduction, *Rare Met.*, 2023, **42**, 1778–1799.

24 I. L. Balasooriya, J. Chen, S. M. Korale Gedara, Y. Han and M. N. Wickramaratne, Applications of nano hydroxyapatite as adsorbents: A review, *Nanomaterials*, 2022, **12**, 2324.

25 (*a*) A. Fihri, C. Len, R. S. Varma and A. Solhy, Hydroxyapatite: A review of syntheses, structure and applications in heterogeneous catalysis, *Coord. Chem. Rev.*, 2017, **347**, 48–76; (*b*) Y. P. Sun, H. Y. Fu, D. L. Zhang, R. X. Li, H. Chen and X. J. Li, Complete hydrogenation of quinoline over hydroxyapatite supported ruthenium catalyst, *Catal. Commun.*, 2010, **12**, 188–192; (*c*) M. Hua, J. Song, C. Xie, H. Wu, Y. Hu, X. Huang and B. Han, Ru/hydroxyapatite as a dual-functional catalyst for efficient transfer hydrogenolytic cleavage of aromatic ether bonds without additional bases, *Green Chem.*, 2019, **21**, 5073–5079; (*d*) M. Pashaei and E. Mehdipour, Silver nanoparticles supported on ionic-tagged magnetic hydroxyapatite as a highly efficient and reusable nanocatalyst for hydrogenation of nitroarenes in water, *Appl. Organomet. Chem.*, 2018, **32**, e4226; (*e*) M. Othmani, H. Bachoua, Y. Ghandour, A. Aissa and M. Debbabi, Synthesis, characterization and catalytic properties of copper-substituted hydroxyapatite nanocrystals, *Mater. Res. Bull.*, 2018, **97**, 560–566; (*f*) H. Tounsi, S. Djemal, C. Petitto and G. Delahay, Copper loaded hydroxyapatite catalyst for selective catalytic reduction of nitric oxide with ammonia, *Appl. Catal., B*, 2011, **107**, 158–163; (*g*) D. Saha, L. Adak, M. Mukherjee and B. C. Ranu, Hydroxyapatite-supported Cu(I)-catalysed cyanation of styrenyl bromides with $K_4[Fe(CN)_6]$: an easy access to cinnamonitriles, *Org. Biomol. Chem.*, 2012, **10**, 952–957.

26 Q. N. Wang, X. F. Weng, B. C. Zhou, S. P. Lv, S. Miao, D. Zhang, Y. Han, S. L. Scott, F. Schüth and A. H. Lu, Direct, selective production of aromatic alcohols from ethanol using a tailored bifunctional cobalt–hydroxyapatite catalyst, *ACS Catal.*, 2019, **9**, 7204–7216.

27 (*a*) H. P, S. Hati and R. Dey, S-Alkylation of dithiocarbamates *via* a hydrogen borrowing reaction strategy using alcohols as alkylating agents, *Org. Biomol. Chem.*, 2023, **21**, 6360–6367; (*b*) V. M, H. P, P. R and R. Dey, Accessing 2-aryl quinolines via acceptorless dehydrogenation and transfer hydrogenation under base and solvent-free reaction conditions, *ChemistrySelect*, 2023, **8**, e202304147; (*c*) H. P, V. M, M. Tomasini, A. Poater and R. Dey, Transition metal-free synthesis of 2-aryl quinazolines *via* alcohol dehydrogenation, *J. Mol. Catal.*, 2023, **542**, 113110–113120; (*d*) H. P, M. Tomasini, V. M, A. Poater and R. Dey, Access to secondary amines *via* the hydrogen auto-transfer reaction mediated by KO$^t$Bu, *Eur. J. Org Chem.*, 2024, e202301213.

28 N. Jamwal, M. Gupta and S. Paul, Hydroxyapatite-supported palladium (0) as a highly efficient catalyst for the Suzuki coupling and aerobic oxidation of benzyl alcohols in water, *Green Chem.*, 2008, **10**, 999–1003.

29 J. Kamieniak, E. Bernalte, C. W. Foster, A. M. Doyle, P. J. Kelly and C. E. Banks, High yield synthesis of hydroxyapatite (HAP) and palladium doped HAP *via* a wet chemical synthetic route, *Catalysts*, 2016, **6**, 119.

30 M. Sudhakar, V. V. Kumar, G. Naresh, M. L. Kantam, S. K. Bhargava and A. Venugopal, Vapor phase hydrogenation of aqueous levulinic acid over hydroxyapatite supported metal (M = Pd, Pt, Ru, Cu, Ni) catalyst, *Appl. Catal., B*, 2016, **180**, 113–120.

31 (*a*) J. Mishra, D. S. Pattanayak, A. A. Das, D. K. Mishra, D. Rath and N. K. Sahoo, Enhanced photocatalytic degradation of cyanide employing Fe-porphyrin sensitizer with hydroxyapatite palladium doped $TiO_2$ nano-composite system, *J. Mol. Liq.*, 2019, **287**, 110821; (*b*) C. Li, G. Xu, X. Liu, Y. Zhang and Y. Fu, Hydrogenation of biomass-derived furfural to tetrahydrofurfuryl alcohol over hydroxyapatite-supported Pd catalyst under mild conditions, *Ind. Eng. Chem. Res.*, 2017, **56**, 8843–8849.

32 D. R. Abernethy, A. J. DeStefano, T. L. Cecil, K. Zaidi and R. L. Williams, Metal impurities in food and drugs, *Pharm. Res.*, 2010, **27**, 750–755.